

Modeling of the Bioactivated Nanopore Devices

AmirAli H. Talasaz, Yang Liu, Mostafa Ronaghi, and Ronald W. Davis

Abstract— This paper presents the modeling of the electrical properties of bioactivated nanopores, customized nanopore devices with a biological macromolecule attached in the pore as the probe. These devices are capable of detecting and analyzing interactions between the attached biomolecule and the molecules in the analyte at a single molecule level.

I. INTRODUCTION

Although nanopore-based sensors have long been explored for single nucleic acid molecule sequencing [1], the researchers still cannot claim success. Nonetheless, nanopores offer one of the most promising approaches for structural analysis of single molecules with a diameter of a few nanometers. Nanometer-scale pores provide an electronic way of probing the structure of a single biomolecule. Bioactivated nanopores have many significant potential applications for bio-analysis in a label-free platform at the single molecule level. Any chemical binding or minor structural changes in the biomolecule can be detected by monitoring the ionic current passing through the nanopore. As a result, these devices can be used to detect the interactions between the biomolecule attached in the pore and the molecules in the analyte at the single molecule level.

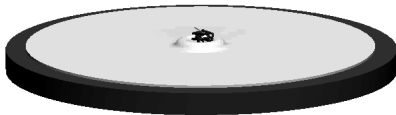


Fig. 1. View of a typical Bioactivated Nanopore in which a biological macromolecule is attached to the nanopore.

In this paper, we describe the fabrication of the bioactivated nanopores in Section II. In Section III, we discuss about electrical modeling of the bioactivated nanopores. We simulate the I-V characteristic of the bioactivated nanopore and the change of the electrical property due to structure change of the probe molecule in catalysis.

Manuscript received Apr, 2006. This research was in part supported by NSF in support of the Network for Computational Nanotechnology (NCN) and National Institute of Health.

A. H. Talasaz is with the Electrical Engineering Department, Stanford University and Stanford Genome Technology Center, CA 94305 USA (corresponding author to provide phone: 650-812-1974; fax: 650-812-1975; e-mail: atalasaz@stanford.edu).

Y. Liu is with the Electrical Engineering Department, Stanford University 94305, CA 94305 USA (e-mail: yangliu1@stanford.edu).

M. Ronaghi is with the Stanford Genome Technology Center, CA 94305 USA (e-mail: mostafa@stanford.edu).

R. W. Davis is with the Stanford Genome Technology Center, CA 94305 USA (e-mail: dbowe@stanford.edu).

II. DEVICE DESIGN AND FABRICATION

The practical implementation of a nanopore-based instrument will likely require the involvement of synthetic nanofabricated pores for increased robustness. Synthetic pores can be fabricated in silicon nitride or silicon oxide membranes using ion-milling as reported in previous works [2]. Silicon nitride membranes possess adequate mechanical strength and are inert to aggressive chemicals. Reproducible 100nm pores have been milled in silicon nitride nanomembranes with a thickness of 45nm. Gold sputtering has been employed as an additional step to decrease the pre-known drilled pore size to the desired value. Gold overhangs formed during sputtering help form low-aspect ratio pores suitable for single-molecular bioactivated nanopore sensors.



Fig. 2. Cross section schematic of the customized Nanopore. Biological macromolecules can be attached on the gold.

Circular low-stress silicon nitride membranes were fabricated. The thickness of the film is 45nm and its diameter is 50 μ m. A dual-FIB system with a 30-kV gallium

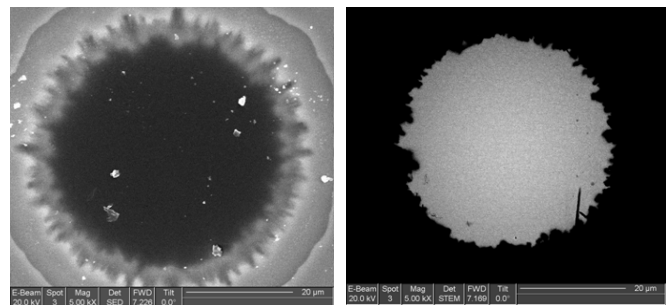
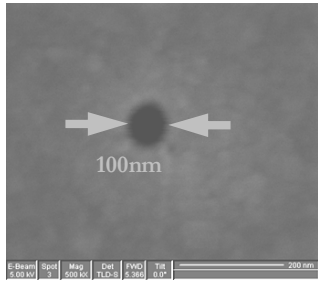
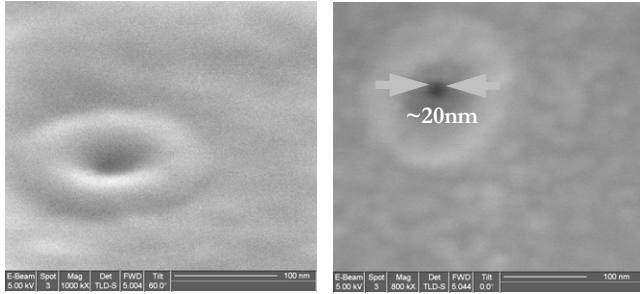


Fig. 3. (Left) Scanning secondary electron microscopy (SEM) (Right) Scanning tunnelling electron microscopy (STEM)

beam is used to drill the pores in the nanomembrane and a circular hole inside the membrane is formed. The size of the FIB-drilled nanopore in the membrane was further reduced to 20nm by gold film sputtering.



(a)



(b)

(c)

Fig. 4. (a) SEM image of a pore milled in silicon nitride membrane before gold sputtering. (b) SEM image of 20nm nanopore in the silicon nitride membrane (60° tilted sample), after sputtering. (c) SEM image of 20nm nanopore (top view)

Silicon nitride is practically inert for biomolecule attachment; while on gold, further surface chemistry modifications can be performed through forming self-assembled monolayers (SAMs) of alkanethiols. Nanopores can be bioactivated through covalent immobilization of biological macromolecules, like antibodies, proteins or DNA single strands in the pore through covalent binding to the SAM. In addition, the nanopore wetting issue is minimized in the customized nanopore device since the nanochannels are in ultra-hydrophilic gold thin films.

III. MODELING

Use of molecular dynamics (MD) simulations to model the electrical properties of the bioactivated nanopore has proven very time-consuming, particularly for large molecules. Thus, given the difficulty of experimental determination and existing MD methods, we propose an alternative approach based on continuum modeling of the protein/nanopore structure with the external electric field applied across nanopores. Such an approach offers a useful solution for efficient bioengineering system simulation with relatively modest computational requirements.

Generally, at the interface of the probe molecule and the solution forms an electrical double layer (EDL) that contains a net excess of mobile ions with a polarity opposite to that of the protein charge. Accordingly, upon applying an external field across the nanopore, the structure of EDL reforms and the distribution of the ions in the nanopore changes. Consequently, the conductivity of the nanopore changes. In

spite of the fact that upon applying external field, the polar groups of the protein may rearrange themselves to maximize the electrostatic attraction, in this simple model, we neglect the effect of the electrical field on protein structure and thus do not account for motions due to internal degrees of freedom, which would result in changes of conformation.

The continuum-based approach is valid to model the ionic current conduction in the protein/nanopore system under study. The pore size is in the tens of nanometer range; therefore the finite ion and water molecule sizes can be neglected. Due to the applied external bias, the entire system is under non-equilibrium condition; the electrostatic potential and the distribution of the ion concentration at each lattice point are calculated by solving the set of Poisson-Nernst-Planck (PNP) equations:

$$\nabla \cdot \epsilon \nabla \psi + (C^+ - C^- + \delta\rho) = 0 \quad (1)$$

$$\frac{\partial C^+}{\partial t} - \nabla \cdot [D^+ \nabla C^+ + \mu^+ C^+ \nabla \psi] = 0 \quad (2)$$

$$\frac{\partial C^-}{\partial t} - \nabla \cdot [D^- \nabla C^- - \mu^- C^- \nabla \psi] = 0 \quad (3)$$

where $\psi(r)$ is the electrostatic potential, $\epsilon(r)$ the dielectric constant, $\delta\rho$ the fixed charge density, $D^{+/-}$ the ion diffusion coefficients, $\mu^{+/-}$ the ion mobilities, and C^+ and C^- cation and anion densities, respectively.

The PNP equations are numerically solved using a general partial differential equation solver, PROPHET [3]. PROPHET provides a script-based programming framework for the assembly and solution of nonlinear PDEs in three-space dimensions and time. The PDEs that can be solved by PROPHET include the elliptic (Poisson) type, diffusion-advection-reaction type, and their combination. Such capabilities make it a particularly suitable numerical tool for continuum-based modeling of non-equilibrium transport as well as equilibrium electrostatics in bioelectrical systems. Previously, PROPHET has been used extensively in the modeling and simulation of semiconductor-based processes [4] and devices [5]. It has recently been applied to solve coupled Poisson-Nernst-Planck equations in the modeling of charge transport in *ompF* porin ion channels [6]. In the current case, the protein and nanopore are not accessible to the electrolytes. Therefore, the PNP equations are solved only in the solution while the Poisson equation is solved inside the protein and membrane. The continuity of electrostatic potential is imposed at the solution/protein and solution/nanopore interfaces. The boundary conditions imposed at the two ends of the pores are such that the potential is equal to the applied voltage bias and the ion concentrations are equal to the equilibrium values. The simulations are carried out on uniform meshes of 2\AA resolution in each direction. The salt concentration is assumed to be 100mM and the dielectric constant of the

protein, nanopore and the solution are 2, 4 and 80 respectively.

The probe molecule we used is myokinase, an enzyme with huge hinge bending. The structure of the enzyme in native state and during catalysis is shown in Fig. 5. The red and green domain is the domain which involves in the interaction with nanopore and was found as described in [7]. Therefore this domain is aligned in the structure of the enzyme in native and catalysis states as shown in figure 5. The white and blue residues, the native structure and during catalysis, are also depicted in figure 5. Intuitively, the nanopore blockage during the catalysis should be larger than in the native structure since the enzyme opens up its structure during catalysis. The numerical simulation of the nanopore/enzyme system confirms this intuition.

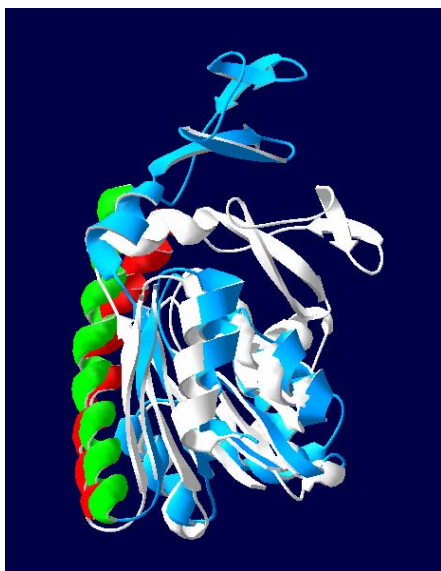
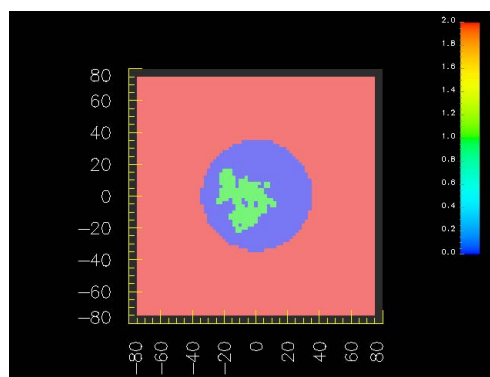
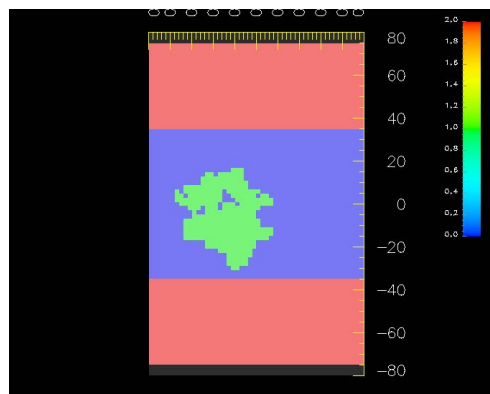


Fig. 5. The 3-D structure of the myokinase at native state and the state during catalysis. The structures are downloaded from Protein Data Bank (PDB IDs: 1ake and 4ake)

The atomic structure of the protein is defined by assigning each atom a radius and the charge distribution inside the protein is represented by a collection of delta functions located at the nucleus of consisting atoms. Radius and partial charges for the protein atoms were assigned using the PDB2PQR web server [8] based on the parameters of the AMBER99 force field [9]. Finally, the protein/nanopore model is then mapped onto a three-dimensional lattice of points. The structure of the bioactivated nanopore which defined for PROPHET, is shown in the following figure.



(a)



(b)

Fig. 6. (a) The top view (b) The cross section of the bioactivated nanopore. The diameter and the length of the nanopore are 10nm.

The mean distribution of the cations and anion are numerically calculated by PROPHET for different voltages applied across the nanopore. Consequently, the conductivity of the nanopore is finally estimated.

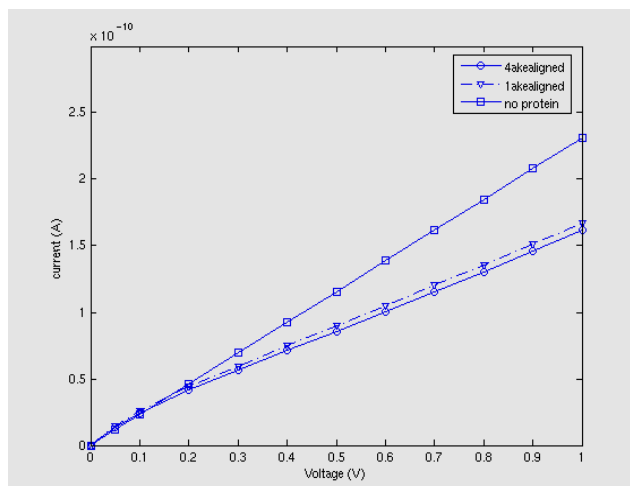


Fig. 7. The I-V characteristic of the nanopore and bioactivated nanopore in native state and during catalysis.

As shown in figure 7, for low voltages, the I-V curve is nonlinear; which is logical due to the nonlinear behavior of the EDL at the protein/ solution interface. For larger voltage, the I-V curve is almost linear since the effect of the protein

partial charges are negligible. As shown in the above figure, the current blockage due to bioactivation of the nanopore is about 50% and the current blockage during catalysis is about 10%, which may be easily detectable in experiments.

It is worth it to mention that in the above simulation, the surface of the nanopore is assumed to be electroneutral. In practice, the zeta potential and consequently the surface charge of the nanopore might be nonzero. However, the surface charge of the nanopore can be easily considered.

III. DISCUSSION

We showed that bioactivated nanopores are one of the most promising approaches to electronically probe the structure of single biomolecules and chemical binding at the single-molecule level. We discussed the electrical modeling of the bioactivated nanopores. We are currently working on experimental data gathering to validate our modeling.

Generally, the modeling of the bio-semiconductor mixed systems is very valuable for the design of the biosensors and biodevices.

ACKNOWLEDGMENT

The authors want to thank Dr. Mohsen Nemat-Gorgani and Prof. Robert Dutton for insightful technical comments and feedbacks.

REFERENCES

- [1] G. Church *et al*, *Characterization of individual polymer molecules based on monomer-interface interactions*, US Patent Specification 5,795,782, 1998.
- [2] J. Li, D. Stein, C. McMullan, D. Branton, M. Aziz, J. A. Golovchenko, "Ion-beam sculpting at nanometre length scales", *Nature*, vol. 412, pp.166-169, 2001.
- [3] <http://www-tcad.stanford.edu/~prophet>.
- [4] M. R. Pinto, D. M. Boulin, C. S. Rafferty, R. K. Smith, J. W. M. Coughran, I. C. Kizilyalli, and M. J. Thoma, in *IEDM Tech. Dig.*, pp. 923-926, 1992
- [5] C. S. Rafferty, B. Biegel, Z. Yu, M. G. Ancona, J. Bude, and R. W. Dutton, in *Simulation of Semiconductor Processes and Devices*, pp. 137-140, 1998
- [6] T. A. Van Der Straaten, J. M. Tang, U. Ravaioli, R. S. Eisenberg, and N. R. Aluru, *J. Comp. Elec.*, vol. 2, pp. 29-47, 2003.
- [7] A. H. Talasaz, M. Nemat-Gorgani, Y. Liu, P. Stahl, M. Ronaghi, and R.W. Davis, "Prediction of the Protein Orientation upon Immobilization on Biological and Non-biological Surfaces", unpublished
- [8] T. J. Dolinsky, J. E. Nielsen, J. A. McCammon, and N. A. Baker, *Nucleic Acids Res.* vol. 32, pp. 665-667, 2004.
- [9] J. M. Wang, P. Cieplak and P. A. Kollman, *J. Comput. Chem.*, vol. 21, pp. 1049-1074, 2000.